BMC Oral Health

RESEARCH

Open Access

Deep learning-based 3D automatic segmentation of impacted canines in CBCT scans

Türkan Ünal[1], Alican Kuran[2], Ibrahim Tevfik Gulsen[3], Fatma Nur Kızılay[4*], Emine Gulsen[1], Semanur Özüdoğru[5], Kadir Gördeli[6], Ozer Celik[7], Mehmet Uğurlu[8], İbrahim Şevki Bayrakdar[9] and Kaan Orhan[10]

Abstract

Background Impacted canines are one of the most frequently encountered dental anomalies in maxillofacial practice. Accurate localization of these teeth is crucial for treatment planning, and Cone Beam Computed Tomography (CBCT) offers detailed 3D imaging for this purpose. However, manual segmentation on CBCT scans is time-consuming and subject to inter-observer variability. This study aimed to develop a deep learning model based on nnU-Net v2 for the automatic segmentation of impacted canines and to evaluate its performance using both classification and segmentation metrics.

Methods A total of 159 CBCT scans containing impacted canines were retrospectively collected and annotated using web-based segmentation software. Model training was performed using the nnU-Net v2 architecture with a learning rate of 0.00001 for 1000 epochs. The performance of the model was evaluated using recall and precision. In addition, segmentation performance was assessed using Dice Similarity Coefficient (DSC), 95% Hausdorff Distance (95% HD in mm), and Intersection over Union (IoU).

Results The nnU-Net v2 model achieved high performance in the detection and segmentation of impacted canines. The values obtained for recall and precision 0.90 and 0.82, respectively. The segmentation metrics were also favorable, with a DSC of 0.84, 95% HD of 7.07 mm, and IoU of 0.74, indicating good overlap between predicted and reference segmentations.

Conclusions The results suggest that the nnU-Net v2-based deep learning model can effectively and autonomously segment impacted canines in CBCT volumes. Its strong performance highlights the potential of artificial intelligence to improve diagnostic efficiency in dentomaxillofacial radiology.

Keywords Artificial intelligence, CBCT, Deep learning, Impacted canine

*Correspondence:
Fatma Nur Kızılay
ftmnr_hrrl@hotmail.com

Full list of author information is available at the end of the article

Introduction

A tooth that has reached its physiological eruption time but fails to take its place in the arch, remaining within the bone tissue due to closure of the root apex, inactivation of the periodontal ligament, and loss of eruptive force, is defined as impacted [1, 2]. The most frequently impacted teeth in the jaws are third molars, followed by canines. However, among canines, maxillary canines tend to remain impacted at a much higher rate compared to mandibular canines, and mandibular canine impaction has been studied less extensively [3, 4]. The prevalence of maxillary canine impaction has been reported to range between 0.97% and 7.10% [5–8], whereas mandibular canine impaction has been reported between 0.3% and 2.8% [9–12]. Bilateral cases have been reported in 8% of patients with impacted maxillary canines [13]. Although the existing literature generally reports the prevalence of unilateral cases for mandibular canine impaction, one study has noted that the distribution of bilateral and unilateral impactions is almost equal [14].

Maxillary and mandibular canines can become impacted as a result of reasons such as obstruction by nearby hard tissues, the presence of local pathology, deviation or disruption of the normal development of the incisors, and hereditary or genetic factors [15]. The canines' proper function and appearance have a substantial impact on the individual's facial characteristics and serve a crucial part in establishing functional occlusion [16]. In addition to concerns related to appearance and functionality, complications such as displacement of nearby teeth and resulting shift in the midline, loss of vitality in neighbouring teeth, development of follicular cysts, ankylosis, recurring infections, pain, resorption of adjacent teeth or the tooth itself, can occur individually or in combination [13]. From this perspective, early recognition of impacted canines serves as an essential factor in eliminating impaction [16]. Several treatment methods have been suggested for this objective, however, the age of the patient and the severity of the impacted canine at the time of diagnosis can influence the effectiveness of early intervention [17]. Therefore, the most efficient approach is to detect and prevent potential impaction at an early stage. In addition, it is necessary to consider surgical exposure and orthodontics in certain situations [16].

It is of great importance to determine the position, angulation, and position of the impacted canines in relation to the buccal or lingual direction in detail, as this will help to determine whether the patient will benefit from a surgical or orthodontic approach [18]. In order to achieve this, both clinical and radiographic examination can be performed to determine the exact localisation. However, radiographs are more useful in this regard since provide a suitable image for the evaluation of impacted canines [16]. In this context, a variety of two-dimensional radiographic techniques, including panoramic radiographs, lateral cephalometric radiographs, anteroposterior radiographs, periapical radiographs, and occlusal radiographs, can assist in the assessment of the position of the canines [19]. Two-dimensional radiographs play a significant role in the early detection of impacted canines, facilitate the treatment and follow-up process due to their low radiographic dose and low cost of availability. Nevertheless, two-dimensional images may occasionally prove inadequate for the precise estimation of the spatial position of impacted teeth within the jaw and for the evaluation of the surrounding anatomical structures. In such instances, cone beam computed tomography (CBCT) becomes a valuable tool for enabling the detailed visualisation of the position of impacted canines and the evaluation of their relationship with neighbouring teeth in the horizontal, vertical, and sagittal axes [20–23].

Digital dentistry is a rapidly developing field, with the incorporation of artificial intelligence into medical imaging leading to the development of CBCT, intraoral and facial scanners, and dental 3D printing. These technologies have the potential to increase the efficiency of dentists and improve the accuracy of orthodontic diagnoses, treatment planning, and surgical guidelines [24]. In this context, segmentation of teeth in CBCT images is a necessary step in the planning of tooth arrangement and stimulation of tooth movement in the digital space. However, in the rapidly developing technological world, performing these procedures manually can be time-consuming, laborious, and may also vary according to intra- and inter-observer variability, which depends on the observers performing the segmentation [25]. Three-dimensional automatic segmentation of impacted canine teeth in CBCT volumes can facilitate the challenging treatment procedure and enhance the certainty and visibility of therapy for clinicians and patients.

A number of studies have been conducted in the field of automatic three-dimensional segmentation of various anatomical structures in CBCT volumes and this area of research is becoming increasingly popular. Several studies have been conducted on automatic segmentation of teeth [24], dental pulp [26], upper respiratory tract [27], mandibular canal [28], maxillary sinus [29, 30], maxilla, and the mandible [31] in CBCT scans. However, the number of studies on automatic segmentation of impacted canine teeth is very limited. While there are studies on the detection and classification of impacted canines on panoramic radiographs [16, 32], there is only one study on the segmentation of impacted canines on CBCT volumes. Swaity et al. [33] employed two 3D U-Net architectures in the training of the convolutional neural network (CNN) model they developed in this direction and reported that the model they developed

demonstrated high performance with a dice similarity coefficient (DSC) of 0.99 ± 0.02. However, it is challenging to ascertain which U-Net configuration is optimal for a given dataset. To address this issue, nnU-Net has developed a range of configurations (2D, 3D full-resolution, 3D low-resolution, 3D cascades) and employs a cross-validation approach to automatically select the most suitable one [34]. This enables users to simply train and apply the models without requiring expertise in this area. nnU-Net is capable of adapting its architectures to the specific image geometry. nnU-Net provides a comprehensive definition of all subsequent steps within the framework. These steps represent the primary determinants of network performance, encompassing pre-processing, training, inference, and potential post-processing [35]. Furthermore, Isensee et al. have demonstrated that the efficacy of the majority of contemporary three-dimensional medical image segmentation methodologies has not surpassed the original nnU-Net baseline success [36].

The objective of this study is to develop a deep learning algorithm based on nnU-Net v2 for the automated segmentation of impacted canines within CBCT volumes and to evaluate its performance. As the majority of CBCT scans in our dataset were obtained from pediatric patients, some images contained metal artefacts due to ongoing orthodontic treatment, while others exhibited motion artefacts because younger patients often have difficulty remaining still during image acquisition. Therefore, we also aimed to investigate whether the presence of such artefacts would affect the segmentation performance of the proposed model. Our first hypothesis is that an nnU-Net v2–based deep learning model can successfully segment impacted canines in CBCT volumes. Our second hypothesis is that the model's segmentation performance will decrease in artefact-affected images compared with artefact-free images.

Material and method

Study design

In this study, a deep learning algorithm based on nnU-net v2 was developed using Craniocatch software (CranioCatch, Eskisehir, Turkey) to automatically segment impacted canine teeth in CBCT volumes of patients in three dimensions. The article for this study was prepared following the Checklist for Artificial Intelligence in Medical Imaging (CLAIM) and the Standards for the Reporting of Diagnostic Accuracy Studies (STARD) Checklist. The study protocol has been authorized by the non-interventional Clinical Research Ethical Committee of Eskisehir Osmangazi University, with decision number 04.10.2022/22. The study was carried out in compliance with the principles outlined in the Declaration of Helsinki.

Sample size calculation

Based on the power analysis conducted to determine the sample size, it was concluded that reliable results could be obtained with 159 CBCT volumes using a paired two-sample t-test, with 95% power and a 5% margin of error, and an effect size of dz = 0.28 (Appendix A) [37, 38].

Patient selection

In this study, CBCT images of patients with unilateral or bilateral impacted canines in the archive of Eskisehir Osmangazi University Department of Oral and Maxillofacial Radiology were evaluated. All patients with impacted canines were included in the study, regardless of the angle or position of the impacted canine. However, the volumes of patients with any pathology (follicular cyst) that would prevent segmentation of the canine tooth in the image were excluded from the study. Both participants without braces and those who did wear braces included in the study, however most of the patients did not have braces. Therefore, patients exhibiting metal artefacts due to orthodontic appliances were also included in the study. Additionally, patients presenting with motion artefacts were likewise integrated into the data set.

A total of 159 CBCT scans were included in the study based on the inclusion and exclusion criteria. Within these scans, 173 impacted canine teeth were identified. Among them, 125 were fully impacted, while 48 were partially erupted. Regarding artefacts, metal artefacts caused by orthodontic brackets or screws were observed in 5 CBCT scans, and motion artefacts were present in 26 scans.

Acquisition of the CBCT volumes

The radiographic images included in the study were obtained on a Planmeca Promax 3D Mid CBCT device (OY, Helsinki, Finland) with a field of view (FOV) scale ranging from 10 × 13 cm to 20 × 17 cm. The images were captured with varying acquisition parameters and voxel sizes of 0.200 mm and 0.400 mm. The patient data was processed into volumetric form and exported as DICOM files, enabling visualization in sagittal, coronal, and axial planes.

Ground truth labelling

The CranioCatch (Eskisehir, Turkey) segmentation module (Fig. 1), a web-based software, was used for the segmentation process. Prior to the manual annotation of ground truth segmentations, the physicians responsible for annotation were first trained both on how to use the segmentation module and to ensure standardization in the annotation process. This training was provided by two researchers: one with 14 years of experience (ISB) and another with 27 years of experience (KO) in the field

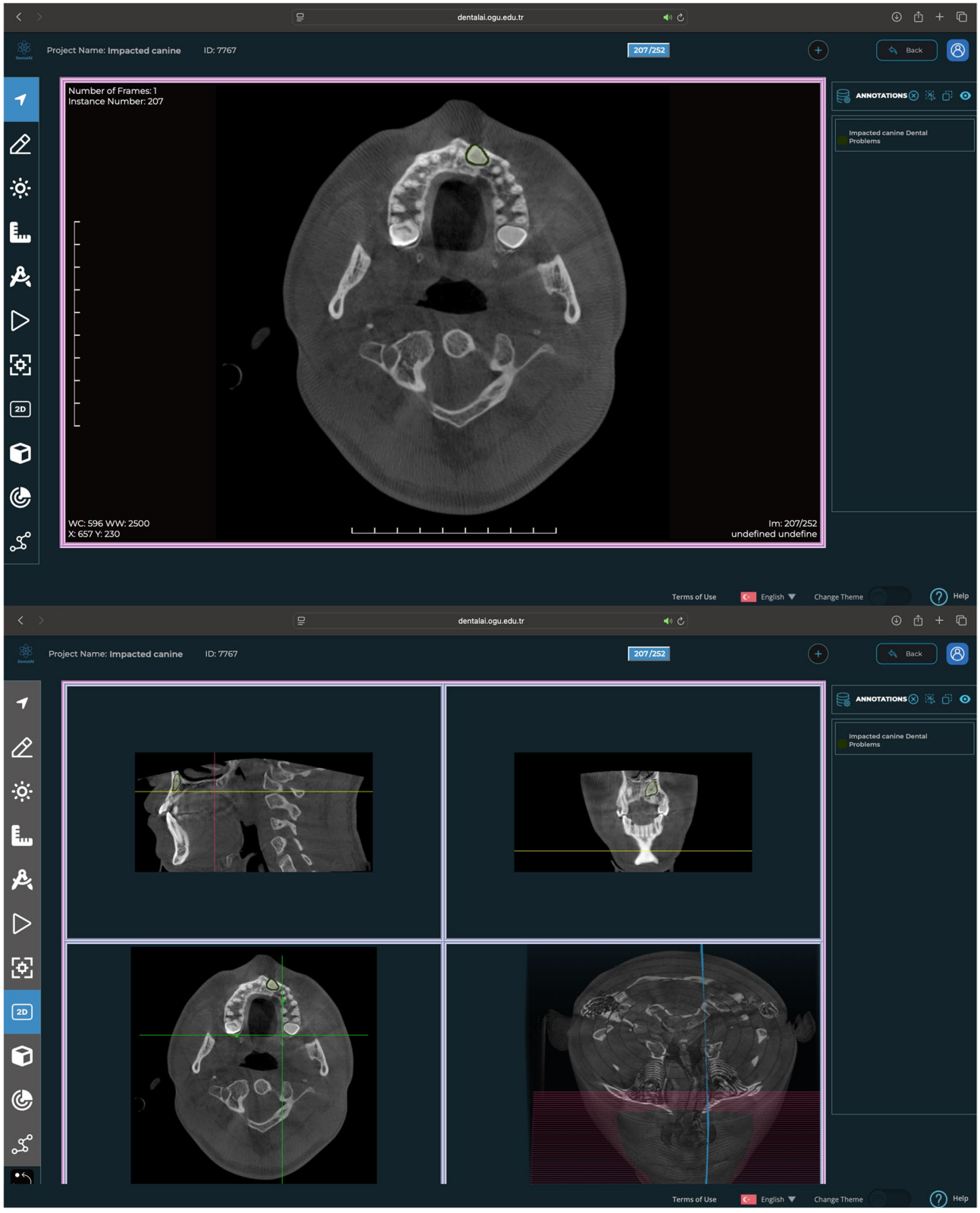

Fig. 1 User interface of the CranioCatch (Eskişehir, Turkey) platform used for web-based manual segmentation of impacted canines to generate ground truth data

of oral and maxillofacial radiology. The trained researchers who performed the annotations, each with 7 years of experience in pediatric dentistry (TM, FNK, EG) and another researcher with 8 years of experience in the same field (SO), completed the manual segmentation process. The segmentations were performed directly on the 3D CBCT volumes using a free-hand segmentation technique. During the annotation process, the accuracy of the segmentations was periodically reviewed by two additional researchers (AK, ITG), each with 4 years of experience in oral and maxillofacial radiology, artificial intelligence, and the use of the CranioCatch segmentation software. After the entire segmentation process was completed, the initial trainers (KO, ISB), both of whom are experienced in their field and knowledgeable in artificial intelligence, reviewed all segmentations. During this review process, the 3D visualization feature of the CranioCatch annotation software (as shown in Fig. 2) enabled thorough examination of the segmentations in sagittal, coronal, and axial planes. Once approved by both reviewers, the ground truth phase was finalized and training of the deep learning algorithm commenced.

Development of the nnU-Net v2 based CNN model

After performing segmentations on a total of 159 CBCT volumes, a hold-out validation strategy was adopted. Specifically, 90% of the dataset (145 CBCT volumes) was used for training, while the remaining 10% (14 CBCT volumes) was set aside as an independent test set. These test images were not seen by the nnU-Net v2 model during training and were reserved exclusively for evaluating its performance. The DICOM files were subsequently converted to the Neuroimaging Informatics Technology Initiative (NIfTI) format utilizing a specialized code developed by the CranioCatch Software Team. This conversion was implemented in Python, leveraging the Pydicom, Nibabel, and OpenCV libraries. In the subsequent step, preprocessing was conducted to standardize the resolution and voxel dimensions across the entire dataset, ensuring consistency prior to model training. This process involved normalizing image intensities to achieve uniformity throughout the dataset, while voxel sizes were resampled to a standardized dimension of $0.4 \times 0.4 \times 0.4$ mm. Additionally, critical hyperparameters for the model's training configuration were defined during this stage. Upon completion of preprocessing, the images were prepared and optimized for the training phase.

The nnU-Net v2 based CNN model for automatic segmentation of impacted canines was developed in Python (v.3.6.1; Python Software Foundation, Wilmington, DE, USA) using the Pytorch, Pydicom, Nibabel, Numpy and Opencv library. The model was trained for 1000 epochs using the Adam optimizer, which is the default configuration in nnU-Net v2. Mathematical processing in the model's training was performed with a Dell PowerEdge T640 Calculation Server (Dell Inc., Round Rock, TX, USA), Dell PowerEdge T640 GPU Calculation Server (Dell Inc., Round Rock, TX, USA), and a Dell PowerEdge R540 Storage Server (Dell Inc., Round Rock, TX, USA) in the Eskişehir Osmangazi University Faculty of Dentistry Dental-AI Laboratory.

The training process of the model is visualized in Fig. 2. When examining the loss/epoch graph, a rapid decrease is observed in both the training loss (loss_tr) and validation loss (loss_val) throughout the training process. In parallel, the pseudo-Dice score, which reflects the model's segmentation accuracy, shows a gradual increase without any notable decline during training. This indicates that the model successfully achieved effective learning. In the time/epoch graph, the duration of each epoch remains relatively constant, demonstrating that the training process proceeded in a computationally stable manner. The learning rate/epoch graph shows that the training began with an initial learning rate of 0.01, which gradually decreased as the number of epochs increased. This reflects the application of a linearly decaying learning rate strategy. The aim of this strategy is to enable the model to learn the impacted canines more rapidly during the early stages with a high learning rate, and in the later stages, to reduce the learning rate to allow for more precise optimization of the network weights—ultimately helping to prevent overfitting.

Evaluation metrics for the model's performance

To evaluate the performance of the developed nnU-Net v2-based model, several key metrics were used, including recall and precision values. Recall and precision values were calculated at the voxel level. Voxels where the model prediction overlapped more than 50% with the ground truth annotation were considered true positives (TP). Voxels predicted as impacted canines by the model but not marked in the ground truth were labelled false positives (FP), while voxels with less than 50% overlap or missed by the model were labelled false negatives (FN). These metrics were computed separately for each impacted tooth, and in cases with multiple impacted canines in a single CBCT, averages were also calculated for the entire volume. Recall and precision were derived from these TP, FP, and FN values. True negatives (TN) were not included because, in voxel-based 3D segmentation, including TN in accuracy calculations can lead to the "accuracy paradox": a large number of voxels not labelled in the ground truth would be counted as TN even if the model underperforms, resulting in misleadingly high accuracy values [33, 39]. Therefore, TN was excluded to provide a more meaningful evaluation of model performance. Furthermore, the Dice Similarity

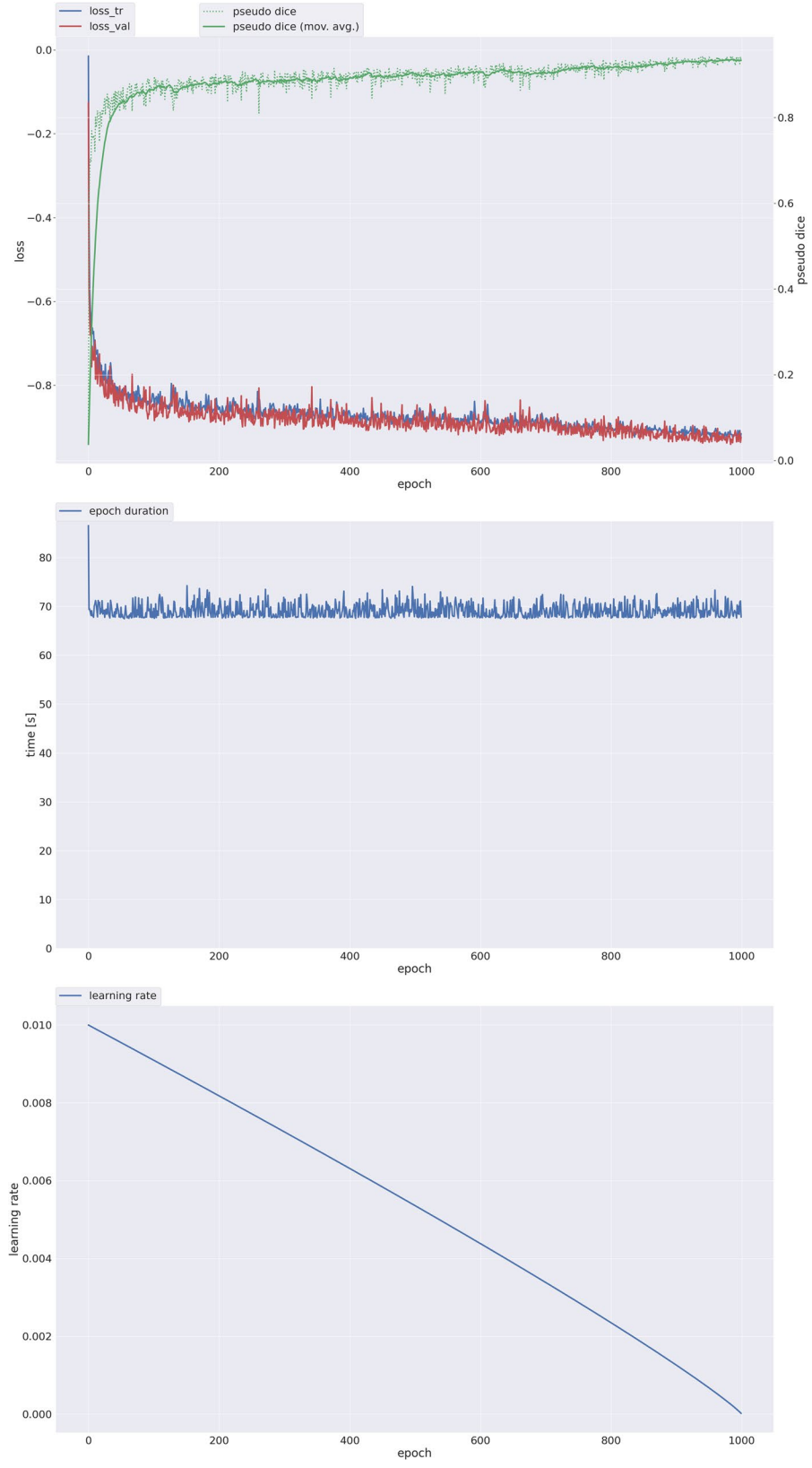

Fig. 2 Deep learning model training progress

Coefficient (DSC), 95% Hausdorff Distance (HD95) (mm), and Intersection over Union (IoU) metrics were employed to assess the efficacy of the model. The DSC value quantifies the number of voxels that exhibit overlap between the ground truth and the segmentation produced by the model at the voxel level. A value of 0 indicates complete dissimilarity, while a value of 1 indicates complete similarity. The HD95 value quantifies the distance between the most distant point in one cluster and the nearest point in the other cluster, and vice versa. A lower value indicates a superior spatial concordance between the model's segmentation and the ground truth. The IoU value assesses the extent of overlap between the predicted and ground truth regions. A value of 0 indicates no overlap between the predicted and ground truth regions, whereas a value of 1 indicates complete overlap.

Results

The nnU-Net v2-based model developed in this study was found to perform at a level comparable to that of paediatric and dentomaxillofacial radiologists in the automatic segmentation of impacted canines in CBCT volumes. The recall value of the model was found to be 0.90. Also known as the true positive rate, recall refers to the proportion of actual positive cases that are correctly classified as positive. This metric, also referred to as the "probability of detection", is considered particularly important in medical applications, especially in scenarios such as disease prediction. In this context, the model's high recall value indicates that it was able to successfully segment the vast majority of impacted canine cases. In contrast, the model's precision value was found to be lower than its recall, calculated at 0.82. While precision increases as false positives decrease, recall increases as false negatives decrease. Therefore, it can be inferred that although the model successfully identified a high number of true positives, it also produced a certain number of false positive segmentations, which accounts for the precision being lower than the recall. One of the key metrics for evaluating the performance of the model's automatic segmentation is the DSC, which was calculated as 0.84 on average in the test set. The DSC values corresponding to the impacted canine segmentations across 14 CBCT volumes in the test set, along with other relevant details, are presented in Table 1.

Another important metric indicating segmentation performance is the HD95, which was found to be 7.07 mm. Although this value is expected to be as low as possible, its relatively high value in our study indicates a notable deviation between the model's predicted segmentations and the ground-truth boundaries. Despite the high DSC, the primary reason for the elevated HD95 appears to be the model's inability to precisely identify the boundaries of the impacted canines. In particular, it was observed that in partially erupted teeth, scans affected by motion artefacts, and cases involving metal artefacts, the model was not able to delineate the tooth boundaries as accurately as the ground truth. This suggests that, although the model achieves satisfactory volumetric overlap (as indicated by DSC), it still struggles with boundary-level precision (as reflected by HD95. Another parameter that evaluates the volumetric overlap between the model's segmentation output and the ground truth is the IoU, which was calculated to be 0.74. The performance metrics used to evaluate the success of the developed model, along with the results demonstrating the model's effectiveness in impacted canine segmentation, are presented in Table 2. Additionally, Fig. 3 provides a visual comparison between the manual segmentations performed by experts and the automatic segmentations generated by the nnU-Net v2-based model for impacted canines. To generate 3D visualizations of the segmented impacted canines presented in Fig. 3, the model's predicted segmentation masks—initially obtained in NIfTI-format—were imported into the 3D Slicer (version 5.6.1) software platform. 3D Slicer is an open-source application widely used in medical image analysis, offering tools for visualization, segmentation, and export of volumetric data across various formats [40]. Within the software, the segmentation masks were first visualized using the "Show 3D" function under the Segment Editor module. Subsequently, the 3D surfaces were exported in STL format using the "Export to files" option in the Segmentations module.

Discussion

Image segmentation is an important step in the analysis of medical images to identify and determine relevant anatomical structures. Threshold-based segmentation is commonly employed due to its simplicity; nevertheless, it lacks specificity because of the unstable grey values in CBCT images and is easily affected by artifacts [41]. Furthermore, there exists a thresholding limitation since a voxel is classified solely according to its intensity. Consequently, distinguishing low-density or thin-layered bone from the adjacent soft tissue is challenging [42]. Alongside the threshold-based segmentation procedure, manual segmentation is an alternative method that can be utilized. Nonetheless, this procedure requires many hours and becomes exceedingly laborious and time-consuming for practical and routine clinical applications [43]. These constraints cause a significant barrier to the implementation of the segmentation process, a key stage of image processing, in clinical 3D CBCT images. Regarding the challenges associated with CBCT image segmentation process, the three-dimensional segmentation of canines—an essential step in digital orthodontic treatment planning—is similarly affected. Consequently,

Table 1 Test set details and model performance based on quantitative and visual assessments

Test Set Number	Jaw	Eruption Status	Artefact	Dice Coefficient	Visual Performance Evaluation
#1	Maxillary Canine	Partially Erupted	Motion Artefact	0.72	The model's prediction was affected by motion artefacts and the partial eruption of the canine.
#2	Maxillary Canine	Partially Erupted	No-Artefact	0.90	The model predicted the canine accurately.
#3	Maxillary Canine	Partially Erupted	Motion Artefact	0.62	The model incorrectly predicted an inverted central incisor as the impacted canine. Also, the canine apex extended between the sinus and nasal cavity, causing incomplete labeling.
#4	Maxillary Canine	Fully Impacted	No-Artefact	0.91	The model produced a highly accurate prediction with no issues.
#5	Maxillary Canine	Fully Impacted	No-Artefact	0.92	Despite the presence of a nearby odontoma, the model predicted the impacted canine with high success.
#6	Maxillary Canine	Fully Impacted	Motion Artefact	0.79	Prediction was impaired due to motion artefacts.
#7	Maxillary Canine	Fully Impacted	No-Artefact	0.92	The model accurately predicted the canine without any issues.
#8	Maxillary Canine	Partially Erupted	No-Artefact	0.56	The model failed to predict the crown-root junction of the maxillary canine, likely interpreting it as a fully erupted tooth. However, the mandibular canine was predicted successfully.
	Mandibular Canine	Fully Impacted		0.88	
#9	Maxillary Canine	Fully Impacted	No-Artefact	0.85	There is crowding in the anterior mandibular region, causing tooth #43 to appear slightly below the occlusal plane. As a result, the model falsely predicted some portion of tooth #43 as an impacted canine, although no actual impaction is present.
#10	Maxillary Canine #1	Fully Impacted	Metal Artefact (RPE + screws)	0.90	Despite metal artefacts from the RPE appliance and screws, the model successfully predicted the impacted canines.
	Maxillary Canine #2	Fully Impacted		0.85	
	Mandibular Canine	Fully Impacted		0.87	
#11	Maxillary Canine	Fully Impacted	Motion Artefact	0.83	The prediction quality was reduced due to motion artefacts.
#12	Maxillary Canine	Partially Erupted	No-Artefact	0.91	The model successfully predicted a small part of the crown that had emerged from bone and the impacted part.
#13	Mandibular Canine	Full Impacted	No-Artefact	0.88	The apex was near dense sclerotic bone, slightly affecting prediction; otherwise, prediction was excellent.
#14	Maxillary Canine	Full Impacted	No-Artefact	0.92	The model produced a highly accurate prediction.

Table 2 Metrics used to evaluate the performance of the nnU-Net v2 model

Metrics	Mathematic Formula	Results	Unit
True positive (TP)		9998.285714285714	Voxel Count
False positive (FP)		2636.4285714285716	Voxel Count
False negative (FN)		1195.5714285714287	Voxel Count
Recall	$TP/((TP+FN))$	0.90	Ratio
Precision	$TP/((TP+FP))$	0.82	Ratio
Dice Similarity Coefficient (DSC)	$2\lvert A \cap B\rvert/((\lvert A\rvert+\lvert B\rvert))$	0.84	Ratio
95% Hausdorff Distance (HD95)	$d_{H95}(A,B)=max(d_{95}(A,B), d_{95}(A,B))$	7.07	mm
Intersection over Union (IoU)	$(\lvert A \cap B\rvert)/(\lvert A \cup B\rvert)$	0.74	Ratio

the development of an automated segmentation process is necessary to enhance the efficiency of the clinical workflow [33].

The effectiveness of computer-aided approaches for identifying impacted canines utilizing imaging processing techniques has been examined in a few earlier studies in the literature; nevertheless, the accuracy levels of the methods produced in these studies are low. They are highly vulnerable to variations in image quality, making them unreliable for routine clinical practice and for images acquired from several centers [44]. There is only one study in the literature that specifically focuses on the segmentation of impacted canines in three-dimensional CBCT images. In their study, Swaity et al. [33] employed a U-Net-based model and reported a nearly perfect segmentation performance, with a DSC of 0.99 and an exceptionally low HD95 value of 0.04 mm. In contrast, the nnU-Net v2-based model developed in our study achieved a DSC of 0.84 and a HD95 of 7.07 mm. These discrepancies can be attributed to notable differences in

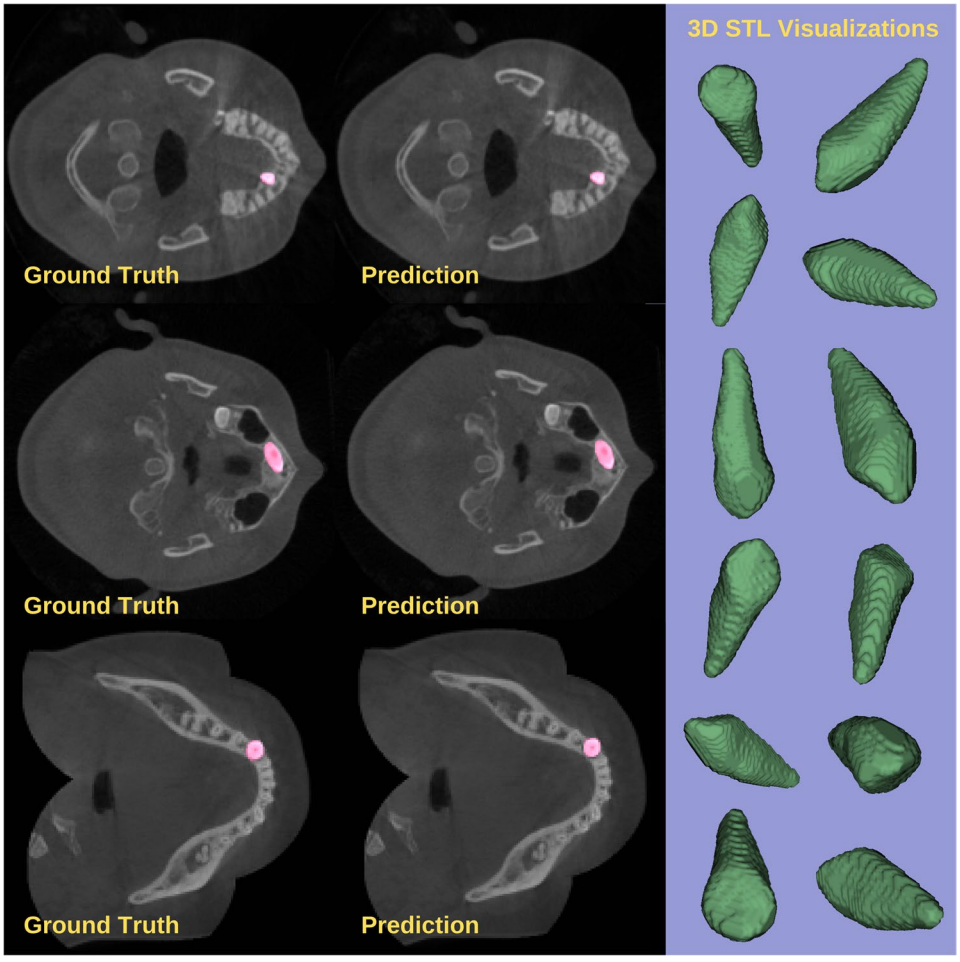

Fig. 3 Comparison between expert-determined ground truth and model predictions in the segmentation of impacted canines, presented with three-dimensional STL visualizations of the model-generated segmentations

both the methodological approaches and dataset characteristics of the two studies. From a methodological standpoint, Swaity et al. [33] fine-tuned a previously trained model — initially designed for segmenting permanent erupted teeth — by introducing impacted canine images. In cases where the model failed to generate accurate results, the outputs were manually refined by experts and used for further training. This semi-automatic refinement process, along with the use of an already optimized model, likely contributed to their highly accurate DSC and nearly flawless HD95 outcomes. In contrast, our study intentionally included images with both metal and motion artefacts, whereas Swaity et al. [33] only included cases with metal artefacts, such as those caused by orthodontic brackets, and explicitly excluded images with motion artefacts. The inclusion of motion artefacts in our dataset was a deliberate choice, as such artefacts are commonly encountered in pediatric patients, where repeated scanning is often avoided to reduce radiation exposure [45, 46]. Therefore, we aimed to evaluate our model's robustness in more clinically realistic conditions. Although Swaity et al. [33] stated that their dataset included partially erupted canines, they did not specify how many of the test cases fell into this category. In contrast, our study provides detailed information about the test set in Table 1, showing that the DSC performance significantly dropped in cases with motion artefacts, while the model achieved DSC values exceeding 0.90 in fully impacted, artefact-free images. Furthermore, unlike the previous study which only targeted maxillary impacted canines, our investigation also included mandibular impacted canines. Our model demonstrated high performance in these cases as well, achieving DSC values approaching 0.90. It was able to successfully segment and detect both maxillary and mandibular impacted canines simultaneously within a single CBCT scan. This can be observed in Case #10 in Table 1. In addition, a qualitative demonstration of the model's segmentation outputs is provided in Fig. 4, illustrating how impacted teeth in both jaws (maxillary and mandibular impacted canines) were accurately segmented within the same CBCT volume of Case #10. Taken together, the relatively lower

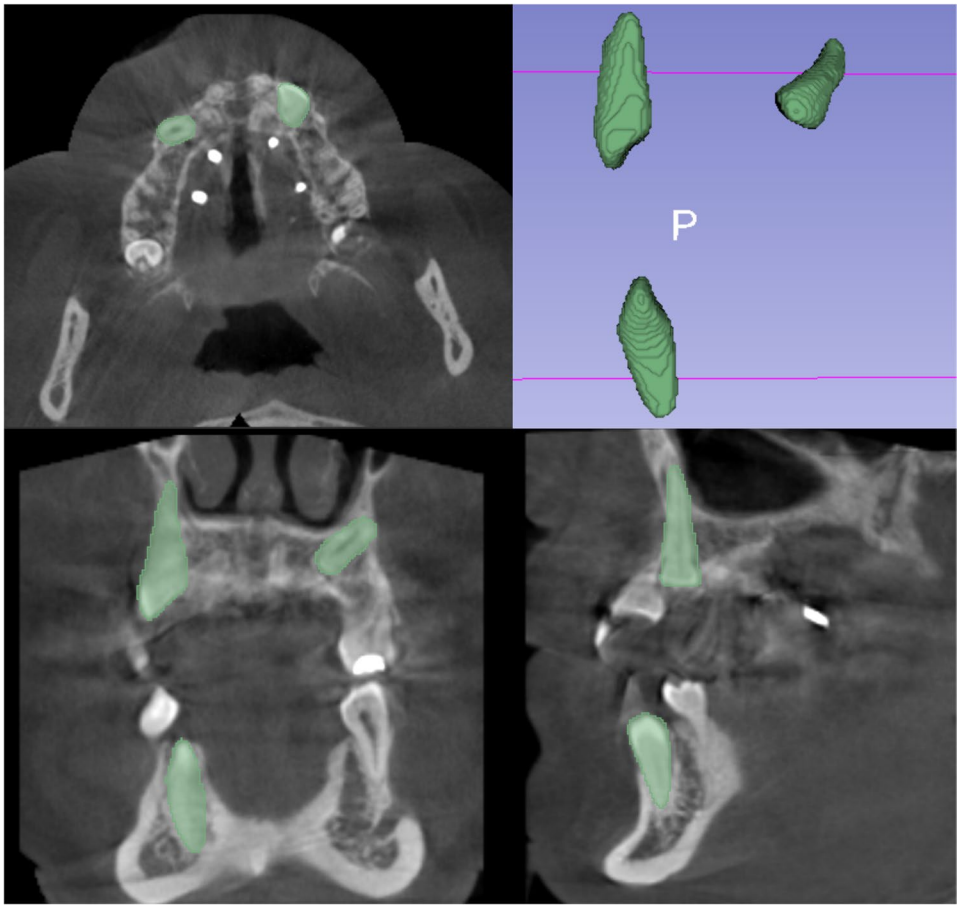

Fig. 4 Qualitative demonstration of the model simultaneously segmenting both maxillary and mandibular impacted canines in Case #10

DSC and higher HD95 values observed in our study can be explained by the increased complexity and variability of our dataset, as well as fundamental differences in methodological design compared to the work by Swaity et al. [33]. In addition to the presence of motion artifacts, other factors influencing the DSC value in this study include the model's misidentification of an inverted impacted central tooth as an impacted canine in one CBCT volume and the incorrect segmentation of a partially impacted canine tooth as fully impacted in another volume (Fig. 5**).** These errors negatively affected the performance metrics, particularly the DSC and IoU values. Nevertheless, despite these challenges, the model demonstrated a high DSC value of 0.84.

In addition to impacted canines, only one other study in the literature has addressed the segmentation of impacted teeth. In their study, Sinard et al. [47] evaluated the accuracy of four deep learning-based tooth segmentation tools on CBCT volumes of patients with multiple impacted teeth. Among these tools, Diagnocat and DentalSegmentator outperformed Relu and CephX across all tested parameters. The reported DSC values ranged from 0.88 to 0.95. However, as their study did not report the HD95, a direct comparison with our HD95 value could not be made. Although Sinard et al. [47] used data from syndromic patients, they did not mention whether any artefacts were present in the CBCT scans. In this context, the average DSC score of 0.84 obtained in our study, demonstrates comparable results to artefact-free cases reported in the literature. Moreover, our model achieved clinically acceptable segmentation performance even on images with artefacts. It is widely accepted in the literature that a DSC score above 0.70 indicates good overlap [48], and in our test set, all but one impacted canine met or exceeded this threshold. Nevertheless, it should be acknowledged that medical segmentation tasks often demand DSC values higher than 0.70 to be considered clinically reliable.

In addition to impacted teeth, numerous studies in the literature have employed deep learning algorithms for the automatic segmentation of normal teeth in CBCT scans. A general review of these studies reveals that the DSC values typically range from 0.90 to 0.97 [49]. Furthermore, there are studies focusing on the automatic segmentation of teeth in CBCT images of pediatric patients during the mixed dentition period—a stage in which both

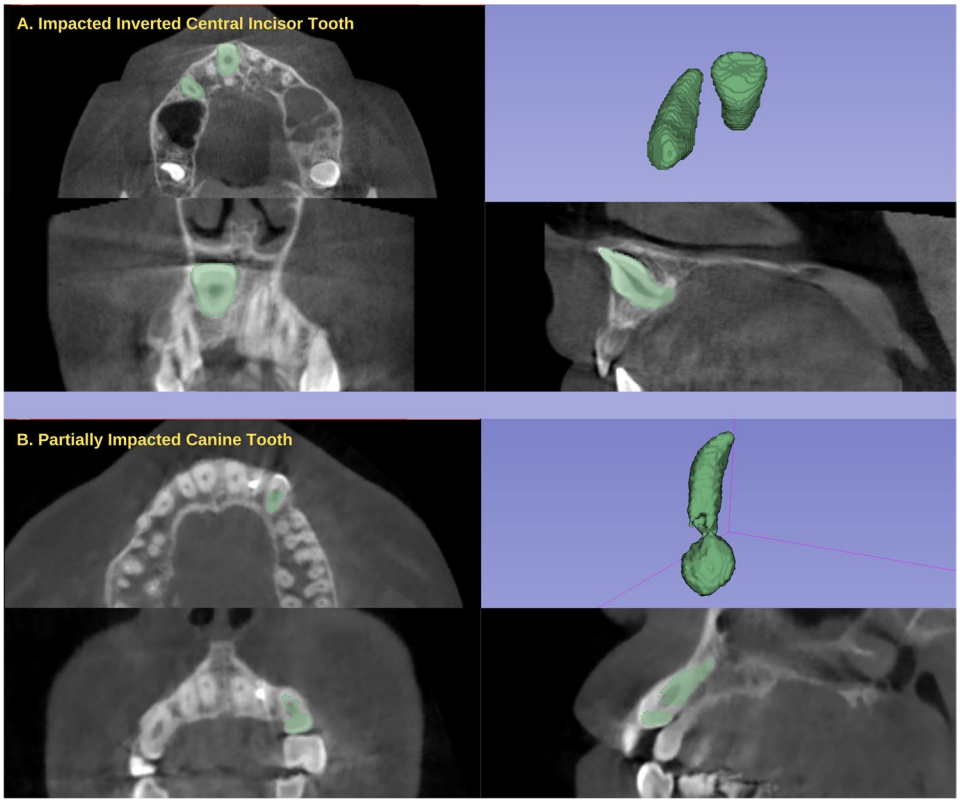

Fig. 5 Examples of CBCT images that have a negative effect on the success of the model. **A** A deep learning model has incorrectly identified an inverted impacted central tooth as an impacted canine. **B** A partially impacted canine tooth has been incorrectly identified as an impacted canine tooth

erupted and unerupted teeth are present. In one such study, Yupeng Hu et al. [50] developed a segmentation algorithm based on the nnU-Net architecture and evaluated it on both internal and external datasets. The model achieved high segmentation performance, with a DSC of 0.96 on the internal dataset and 0.95 on the external dataset. However, a review of the inclusion and exclusion criteria in most of the existing studies reveals a common tendency to exclude CBCT scans with motion or metal artefacts. This is particularly significant in pediatric populations, where maintaining stillness during CBCT acquisition is challenging, often resulting in artefact-laden scans. Our study was specifically designed with this real-world scenario in mind, including such challenging cases, which differentiates it from the majority of prior research. Consequently, the slightly lower DSC values reported in our study are to be expected and should be interpreted in light of this context. Nonetheless, it is noteworthy that in artefact-free scans and in cases of fully impacted canines, the developed model achieved high segmentation performance with DSC values exceeding 0.90. Therefore, our study offers a unique contribution to the literature by adopting a more clinically realistic approach that has not been previously explored, highlighting the model's robustness in scenarios often excluded from prior segmentation studies.

In this study, we developed an nnU-Net v2–based deep learning algorithm capable of automatically segmenting impacted canines with high DSC values even in artifact-affected CBCT scans and achieving DSC values above 0.90 with only minimal errors in artifact-free scans. Such performance enables potential integration into various clinical scenarios and incorporation into digital dentistry workflows, thereby reducing procedure times. With further optimization and minor expert refinements, the model has the potential to provide clinically acceptable, real-world–ready segmentations, which could bring meaningful changes to impacted-canine–related applications in digital dentistry. In particular, STL files generated after automatic segmentation can be used to produce 3D-printed tooth replicas, which—when combined with computer-aided design and manufacturing (CAD/CAM)–fabricated surgical templates—may facilitate guided autotransplantation by allowing the donor tooth to be replicated precisely, tested in the recipient site preoperatively, and thereby reducing extraoral time. Additionally, in the surgical management of impacted canines, patient-specific surgical guides can enable less invasive, shorter, and more controlled extraction/exposure procedures [51]. In orthodontic planning, the 3D model can reveal root orientation and crown-root relationships, supporting preoperative decision-making through digital

simulation. It may also facilitate the design of customized orthodontic appliances or attachments [52]. Therefore, the model we developed not only has the potential to assist clinicians in CBCT interpretation of impacted canines—by enabling the assessment of anatomical configurations and root resorption—but also to enhance efficiency in clinical digital dentistry workflows through automated segmentation.

A key limitation of this study is that the CBCT images used for both training and testing were sourced from a single tomography device. This restriction may limit the model's generalizability to scans from other centers or devices. This study evaluated the performance of only a single deep learning model without comparing how the performance might vary across multiple alternative architectures. The lack of such comparisons with other competitive deep learning approaches represents an important limitation of our work. Additionally, the model was exclusively trained and evaluated on CBCT images of impacted canine teeth, which may have contributed to the incorrect segmentation of an inverted central tooth as an impacted canine. Expanding the model to include multiclass training with CBCT volumes that encompass supernumerary and other types of impacted teeth could enhance its robustness in addressing these commonly encountered scenarios in radiographic examinations.

Conclusion

Artificial intelligence models utilizing deep learning algorithms based on nnU-Net v2 demonstrate performance comparable to that of expert dentists in the segmentation of impacted canine teeth in CBCT scans.

Abbreviations

AI	Artificial intelligence
CBCT	Cone beam computed tomography
CNN	Convolutional neural network
CLAIM	Checklist for artificial intelligence in medical imaging
DICOM	Digital imaging and communications in medicine
DSC	Dice similarity coefficient
FOV	Field of view
95HD	%95 Hausdorff distance
IoU	Intersection over union
NIfTI	Neuroimaging informatics technology initiative
nnU-Net v2	No new-net – universal network version 2
Pydicom	Python DICOM library
STARD	Standards for the reporting of diagnostic accuracy studies

Supplementary Information

The online version contains supplementary material available at https://doi.org/10.1186/s12903-025-07117-5.

Supplementary Material 1.

Acknowledgements

Not applicable.

Clinical trial registration

Not applicable.

Declaration of Helsinki

This study was conducted in accordance with the ethical principles stated in the Declaration of Helsinki.

Authors' contributions

TM, FNK, EG and SÖ performed the image annotationMU assisted in data collection and image processing ITG and AK supervised the labelling process and wrote original manuscriptKG and ÖC developed and implemented the deep learning model and conducted the training experimentsİŞB and KO provided expert supervision, revised the manuscript critically, and ensured overall methodological accuracyAll authors read and approved the final version of the manuscript.

Funding

This research received no specific grant from any funding agency in the public, commercial, or not-for-profit sectors.

Data availability

The CBCT datasets used in this study are not publicly available due to institutional and ethical restrictions on sharing patient-related imaging data. However, they are available from the corresponding author on reasonable request and with permission from the Eskisehir Osmangazi University Non-Interventional Clinical Research Ethics Committee.

Declarations

Ethics approval and consent to participate

Written informed consent was obtained from all participants (or their legal guardians) for the use and publication of their radiological images and anonymized data. The study was approved by the Non-Interventional Clinical Research Ethics Committee of Eskisehir Osmangazi University (Approval No: 04.10.2022/22).

Consent for publication

Not applicable.

Competing interests

Ibrahim Sevki Bayrakdar reports a relationship with CranioCatch that includes: board membership and equity or stocks. Dr. Ibrahim Sevki Bayrakdar is the Co-founder and CEO of CranioCatch, a company specializing in the development of advanced artificial intelligence solutions for use in dentistry and related fields. In his role, he oversees company operations, strategic planning, and product development. Given his professional role and business interests in CranioCatch, there may be a potential conflict of interest regarding the content of this article. While every effort has been made to ensure an objective and balanced perspective, readers are advised to consider this potential influence. Dr. Bayrakdar remains committed to ethical conduct, transparency, and integrity in all academic and professional activities. As other authors, we do not have any conflict of interest to disclose. If there are other authors, they declare that they have no known competing financial interests or personal relationships that could have appeared to influence the work reported in this paper.

Author details

[1]Alanya Oral and Dental Health Center, Antalya, Turkey
[2]Department of Oral and Maxillofacial Radiology, Faculty of Dentistry, Kocaeli University, Kocaeli, Turkey
[3]Department of Oral and Maxillofacial Radiology, Faculty of Dentistry, Alanya Alaaddin Keykubat University, Antalya, Turkey
[4]Department of Pediatric Dentistry, Faculty of Dentistry, Inonu University, Malatya, Turkey
[5]Department of Pediatric Dentistry, Faculty of Dentistry, Istanbul Medeniyet University, Istanbul, Turkey
[6]Eskişehir Oral and Dental Health Center, Eskisehir, Turkey
[7]Department of Mathematics-Computer, Faculty of Science, Eskisehir Osmangazi University, Eskisehir, Turkey
[8]Department of Orthodontics, Faculty of Dentistry, Eskisehir Osmangazi University, Eskisehir, Turkey

[9]Department of Oral and Maxillofacial Radiology, Faculty of Dentistry, Eskisehir Osmangazi University, Eskisehir, Turkey
[10]Department of Oral and Maxillofacial Radiology, Faculty of Dentistry, Ankara University, Ankara, Turkey

Received: 26 June 2025 / Accepted: 3 October 2025
Published online: 23 December 2025

References

1. Litsas G, Acar A. A review of early displaced maxillary canines: Etiology, diagnosis and interceptive treatment. Open Dent J. 2011;5:39–47. https://doi.org/10.2174/1874210601105010039.
2. Suri L, Gagari E, Vastardis H. Delayed tooth eruption: pathogenesis, diagnosis, and treatment. A literature review. Am J Orthod Dentofac Orthop Off Publ Am Assoc Orthod its Const Soc Am Board Orthod. 2004;126:432–45. https://doi.org/10.1016/j.ajodo.2003.10.031.
3. Guarnieri R, Germanò F, Sottile G, Barbato E, Cassetta M. Local factors relating to mandibular canine impaction: A retrospective study. Am J Orthod Dentofac Orthop. 2024;165:556–64. https://doi.org/10.1016/j.ajodo.2023.11.013.
4. Dalessandri D, Parrini S, Rubiano R, Gallone D, Migliorati M. Impacted and transmigrant mandibular canines incidence, aetiology, and treatment: a systematic review. Eur J Orthod. 2017;39:161–9. https://doi.org/10.1093/ejo/cjw027.
5. Dachi SF, Howell FV. A survey of 3,874 routine full-mouth radiographs: I. A study of retained roots and teeth. Oral Surg Oral Med Oral Pathol. 1961;14:916–24. https://doi.org/10.1016/0030-4220(61)90003-2.
6. Sacerdoti R, Baccetti T. Dentoskeletal features associated with unilateral or bilateral palatal displacement of maxillary canines. Angle Orthod. 2004;74:725–32. https://doi.org/10.1043/0003-3219. (2004)074%253C0725:DFAWUO%253E2.0.CO;2.
7. Celikoglu M, Kamak H, Oktay H. Investigation of transmigrated and impacted maxillary and mandibular canine teeth in an orthodontic patient population. J Oral Maxillofac Surg. 2010;68:1001–6. https://doi.org/10.1016/j.joms.2009.09.006.
8. Mercuri E, Cassetta M, Cavallini C, Vicari D, Leonardi R, Barbato E. Dental anomalies and clinical features in patients with maxillary canine impaction. Angle Orthod. 2013;83(1):22–8. https://doi.org/10.2319/021712-149.1.
9. Sajnani AK, King NM. Impacted mandibular canines: prevalence and characteristic features in Southern Chinese children and adolescents. J Dent Child Am Acad Pediatr Dentistry. 2014;81:3–6.
10. Aras M-H, Halicioğlu K, Yavuz M-S, Çağlaroğlu M. Evaluation of surgical-orthodontic treatments on impacted mandibular canines. Med Oral Patol Oral Cir Bucal. 2011;16:e925–928.
11. Bertl MH, Frey C, Bertl K, Giannis K, Gahleitner A, Strbac GD. Impacted and transmigrated mandibular canines: an analysis of 3D radiographic imaging data. Clin Oral Investig. 2018;22:2389–99. https://doi.org/10.1007/s00784-018-2342-0.
12. Bhullar MK, Aggarwal I, Verma R, Uppal AS. Mandibular canine transmigration: report of three cases and literature review. J Int Soc Prev Community Dent Wolters Kluwer (UK) Ltd. 2017;7:8–14. https://doi.org/10.4103/jispcd.JISPCD_231_16.
13. Bishara SE. Impacted maxillary canines: a review. Soc Am Board Orthod. 1992;101:159–71. https://doi.org/10.1016/0889-5406(92)70008-X. Am J Orthod Dentofac Orthop Off Publ Am Assoc Orthod Its Const.
14. Agastra E, Saettone M, Parrini S, Cugliari G, Deregibus A, Castroflorio T. Impacted permanent mandibular canines: epidemiological evaluation. J Clin Med. 2023;12:5375. https://doi.org/10.3390/jcm12165375.
15. Becker A, Chaushu S. Etiology of maxillary canine impaction: A review. Am J Orthod Dentofac Orthop. 2015;148:557–67. https://doi.org/10.1016/j.ajodo.2015.06.013.
16. Aljabri M, Aljameel SS, Min-Allah N, Alhuthayfi J, Alghamdi L, Alduhailan N, et al. Canine impaction classification from panoramic dental radiographic images using deep learning models. Inf Med Unlocked. 2022;30:100918. https://doi.org/10.1016/j.imu.2022.100918.
17. MacDonald D, Alebrahim S, Yen E, Aleksejuniene J. Cone-beam computed tomographic reconstructions in the evaluation of maxillary impacted canines. Imaging Sci Dent. 2023;53:145–51. https://doi.org/10.5624/isd.20220211.
18. Grisar K, Luyten J, Preda F, Martin C, Hoppenreijs T, Politis C, et al. Interventions for impacted maxillary canines: A systematic review of the relationship between initial canine position and treatment outcome. Orthod Craniofac Res. 2021;24:180–93. https://doi.org/10.1111/ocr.12423.
19. Kumar S, Mehrotra P, Bhagchandani J, Singh A, Garg A, Kumar S, et al. Localization of impacted canines. J Clin Diagn Res JCDR. 2015;9:ZE11–14. https://doi.org/10.7860/JCDR/2015/10529.5480.
20. Alqerban A, Storms A-S, Voet M, Fieuws S, Willems G. Early prediction of maxillary canine impaction. Dentomaxillofacial Radiol. 2016;45:20150232. https://doi.org/10.1259/dmfr.20150232.
21. Alqerban A, Willems G, Bernaerts C, Vangastel J, Politis C, Jacobs R. Orthodontic treatment planning for impacted maxillary canines using conventional records versus 3D CBCT. Eur J Orthod. 2014;36:698–707. https://doi.org/10.1093/ejo/cjt100.
22. Alqerban A, Jacobs R, Fieuws S, Willems G. Comparison of two cone beam computed tomographic systems versus panoramic imaging for localization of impacted maxillary canines and detection of root resorption. Eur J Orthod. 2011;33:93–102. https://doi.org/10.1093/ejo/cjq034.
23. Stewart JA, Heo G, Glover KE, Williamson PC, Lam EW, Major PW. Factors that relate to treatment duration for patients with palatally impacted maxillary canines. Am J Orthod Dentofac Orthop Off Publ Am Assoc Orthod its Const Soc Am Board Orthod. 2001;119:216–25. https://doi.org/10.1067/mod.2001.110989.
24. Jang TJ, Kim KC, Cho HC, Seo JK. A fully automated method for 3D individual tooth identification and segmentation in dental CBCT. IEEE Trans Pattern Anal Mach Intell. 2022;44:6562–8. https://doi.org/10.1109/TPAMI.2021.3086072.
25. Chen Y, Du H, Yun Z, Yang S, Dai Z, Zhong L, et al. Automatic segmentation of individual tooth in dental CBCT images from tooth surface map by a Multi-Task FCN. IEEE Access. 2020;8:97296–309. https://doi.org/10.1109/ACCESS.2020.2991799.
26. Duan W, Chen Y, Zhang Q, Lin X, Yang X. Refined tooth and pulp segmentation using U-Net in CBCT image. Dento Maxillo Facial Radiol. 2021;50:20200251. https://doi.org/10.1259/dmfr.20200251.
27. Alsufyani N, Flores-Mir C, Major P. Three-dimensional segmentation of the upper airway using cone beam CT: a systematic review. Dentomaxillofacial Radiol. 2012;41:276–84. https://doi.org/10.1259/dmfr/79433138.
28. Cipriano M, Allegretti S, Bolelli F, Di Bartolomeo M, Pollastri F, Pellacani A, et al. Deep segmentation of the mandibular canal: A new 3D annotated dataset of CBCT volumes. IEEE Access. 2022;10:11500–10. https://doi.org/10.1109/ACCESS.2022.3144840.
29. Morgan N, Van Gerven A, Smolders A, de Faria Vasconcelos K, Willems H, Jacobs R. Convolutional neural network for automatic maxillary sinus segmentation on cone-beam computed tomographic images. Sci Rep Nat Publishing Group. 2022;12:7523. https://doi.org/10.1038/s41598-022-11483-3.
30. Bayrakdar IS, Elfayome NS, Hussien RA, Gulsen IT, Kuran A, Gunes I, et al. Artificial intelligence system for automatic maxillary sinus segmentation on cone beam computed tomography images. Dentomaxillofacial Radiol. 2024;53:256–66. https://doi.org/10.1093/dmfr/twae012.
31. Wang H, Minnema J, Batenburg KJ, Forouzanfar T, Hu FJ, Wu G. Multiclass CBCT image segmentation for orthodontics with deep learning. J Dent Res SAGE Publications Inc. 2021;100:943–9. https://doi.org/10.1177/00220345211005338.
32. Abdulkreem A, Bhattacharjee T, Alzaabi H, Alali K, Gonzalez A, Chaudhry J, et al. Artificial intelligence-based automated preprocessing and classification of impacted maxillary canines in panoramic radiographs. Dento Maxillo Facial Radiol. 2024;53:173–7. https://doi.org/10.1093/dmfr/twae005.
33. Swaity A, Elgarba BM, Morgan N, Ali S, Shujaat S, Borsci E, et al. Deep learning driven segmentation of maxillary impacted canine on cone beam computed tomography images. Sci Rep Nat Publishing Group. 2024;14:369. https://doi.org/10.1038/s41598-023-49613-0.
34. Isensee F, Jaeger PF, Kohl SAA, Petersen J, Maier-Hein KH. nnU-Net: a self-configuring method for deep learning-based biomedical image segmentation. Nat Methods Nat Publishing Group. 2021;18:203–11. https://doi.org/10.1038/s41592-020-01008-z.
35. Isensee F, Petersen J, Klein A, Zimmerer D, Jaeger PF, Kohl S, et al. nnU-Net: Self-adapting framework for U-Net-based medical image segmentation [Internet]. arXiv; 2018. [cited 2024 May 2]. https://doi.org/10.48550/arXiv.1809.10486.
36. Isensee F, Wald T, Ulrich C, Baumgartner M, Roy S, Maier-Hein KH, et al. nnU-Net revisited: A call for rigorous validation in 3D medical image segmentation. arXiv preprint arXiv: 2404.09556. 2024. https://doi.org/10.48550/arXiv.2404.09556.

37. Cohen J. Statistical power analysis for the behavioral sciences. 2nd ed. New York: Routledge; 1988. https://doi.org/10.4324/9780203771587.
38. Gibson E, Hu Y, Huisman HJ, Barratt DC. Designing image segmentation studies: statistical power, sample size and reference standard quality. Med Image Anal. 2017;42:44–59. https://doi.org/10.1016/j.media.2017.07.004.
39. Valverde-Albacete FJ, Peláez-Moreno C. 100% classification accuracy considered harmful: the normalized information transfer factor explains the accuracy paradox. PLoS ONE. 2014;9:e84217. https://doi.org/10.1371/journal.pone.0084217.
40. Fedorov A, Beichel R, Kalpathy-Cramer J, Finet J, Fillion-Robin J-C, Pujol S, et al. 3D slicer as an image computing platform for the quantitative imaging network. Magn Reson Imaging. 2012;30:1323–41. https://doi.org/10.1016/j.mri.2012.05.001.
41. Pham DL, Xu C, Prince JL. Current methods in medical image segmentation. Annu Rev Biomed Eng. 2000;2:315–37. https://doi.org/10.1146/annurev.bioeng.2.1.315.
42. Zhang J, Yan C-H, Chui C-K, Ong S-H. Fast segmentation of bone in CT images using 3D adaptive thresholding. Comput Biol Med. 2010;40:231–6. https://doi.org/10.1016/j.compbiomed.2009.11.020.
43. Chen S, Wang L, Li G, Wu T-H, Diachina S, Tejera B, et al. Machine learning in orthodontics: introducing a 3d Auto-segmentation and Auto-landmark finder of Cbct images to assess maxillary constriction in unilateral impacted canine patients. Angle Orthod. 2019;90:77–84. https://doi.org/10.2319/012919-59.1.
44. Unleashing hidden canines. : a novel fast R-CNN based technique for automatic auxiliary canine impaction. Int J Adv Technol Eng Explor [Internet]. 2024. https://doi.org/10.19101/IJATEE.2023.10102600. [cited 2024 Oct 17];11.
45. Uzun C, Stelt P, Sumer A, Abacı SH. Diagnostic image quality of digital panoramic radiography of pediatric patients. 2018 [cited 2024 Oct 17]. https://www.semanticscholar.org/paper/Diagnostic-image-quality-of-digital-panoramic-of-Uzun-Stelt/93e88ba57b9b53aeeed016959fbb3f205c88dd86. Accessed 17 Oct 2024.
46. Nahir CB, Çitir M, Çolak S, Keldal G. Assessment of cone beam computed tomography use in pediatric and adolescent patients: a cross-sectional study. BMC Oral Health. 2024;24:1068. https://doi.org/10.1186/s12903-024-04813-6.
47. Sinard E, Gajny L, de La Dure-Molla M, Felizardo R, Dot G. Automated cone beam computed tomography segmentation of multiple impacted teeth with or without association to rare diseases: evaluation of four deep Learning-Based methods. Orthod Craniofac Res. 2025;28:433–40. https://doi.org/10.1111/ocr.12890.
48. Zijdenbos AP, Dawant BM, Margolin RA, Palmer AC. Morphometric analysis of white matter lesions in MR images: method and validation. IEEE Trans Med Imaging. 1994;13:716–24. https://doi.org/10.1109/42.363096.
49. Polizzi A, Quinzi V, Ronsivalle V, Venezia P, Santonocito S, Lo Giudice A, et al. Tooth automatic segmentation from CBCT images: a systematic review. Clin Oral Investig. 2023;27:3363–78. https://doi.org/10.1007/s00784-023-05048-5.
50. Hu Y, Liu C, Liu W, Xiong Y, Zeng W, Chen J, et al. Fully automated method for three-dimensional segmentation and fine classification of mixed dentition in cone-beam computed tomography using deep learning. J Dent. 2024;151:105398. https://doi.org/10.1016/j.jdent.2024.105398.
51. Park S, Lee H, Lee E, Jeong T, Lee H, Shin J. Guided autotransplantation of impacted canines using a CAD/CAM surgical template. Children. 2023;10:708. https://doi.org/10.3390/children10040708.
52. Borohovitz CL, Abraham Z, Redmond WR. The diagnostic advantage of a CBCT-derived segmented STL rendition of the teeth and jaws using an AI algorithm. J Clin Orthod JCO. 2021;55:361–9.

Publisher's note